American Mineralogist, Volume 89, pages 1142–1147, 2004

LETTER

Cation disorder in dolomite, $CaMg(CO_3)_2$, and its influence on the aragonite + magnesite ↔ dolomite reaction boundary

SYTLE M. ANTAO,[1,*] WILLEM H. MULDER,[2] ISHMAEL HASSAN,[2] WILSON A. CRICHTON,[3] AND JOHN B. PARISE[1]

[1]Mineral Physics Institute & Department of Geosciences, State University of New York, Stony Brook, New York 11794-2100, U.S.A.
[2]Department of Chemistry, University of the West Indies, Mona, Kingston 7, Jamaica

ABSTRACT

The structure of dolomite, $CaMg(CO_3)_2$, was determined from 298 to 1466 K at a constant pressure of about 3 GPa using in situ synchrotron X-ray diffraction data to investigate the state of disorder. An order parameter s, defined as $2\,x_{Ca} - 1$, varies from $s = 1$ (where $x_{Ca} = 1$) for a completely ordered dolomite to $s = 0$ (where $x_{Ca} = 0.5$) for a completely disordered dolomite. On heating, there is no measured change in s until the temperature is high enough to cause exchange of Ca^{2+} and Mg^{2+} cations. Significant disorder began to occur at about 1234 K [$s = 0.83(1)$] and increases along a smooth pathway to $T = 1466$ K [$s = 0.12(5)$]. The $R\bar{3} \leftrightarrow R\bar{3}c$ transition in dolomite is described by a modified Bragg-Williams thermodynamic model with the following molar free energy of disorder, $\bar{G}_d(T; s) = RT_c[1 - s^2 + {}^1/_2\, a(s^4 - 1) - (T/T_c)\,\{2\ln 2 - (1+s)\ln(1+s) - (1-s)\ln(1-s)\}]$. Using $T_c = 1466$ K and $a = -0.29$, this model provides an excellent agreement with experimental data. Moreover, the maximum enthalpy of disorder, $\bar{H}_d(s = 0) = RT_c(1 - {}^1/_2\, a) \sim 14$ kJ/mol, agrees with published calorimetric data. A thermodynamic description of the aragonite + magnesite ↔ dolomite reaction boundary is also presented and it reproduces the main qualitative features correctly.

INTRODUCTION

There is interest in the properties of carbonate minerals at high pressures and temperatures because of their important implications for the Earth's carbon cycle, oxygen fugacity, and stability of other minerals in the mantle. Dolomite, $CaMg(CO_3)_2$, is intriguing because the structure contains alternating planes of Ca^{2+} and Mg^{2+} cations, and cation disorder with pressure and temperature significantly affects mineral properties.

The structure of dolomite ($R\bar{3}$) is similar to that of calcite ($R\bar{3}c$), consisting of corner-linked octahedra and nearly planar CO_3^{2-} groups (Fig. 1). The lower symmetry of dolomite results from alternating Ca^{2+} and Mg^{2+} octahedral layers and slight rotation of the CO_3^{2-} groups, which move the oxygen atoms off of the twofold axis that exists in calcite. An order parameter $s = 2x_{Ca} - 1$, describes the degree of order in dolomite (see Reeder and Wenk 1983). The parameter $s = 1$ (where $x_{Ca} = 1$) for complete order and $s = 0$ (where $x_{Ca} = 0.5$) for complete disorder. Rotational disorder may also occur about a specific axis, as observed for CO_3^{2-} groups in some rhombohedral oxides (Ferrario et al. 1994). The charge density effect on the CO_3^{2-} groups is not uniform because of two different cations in adjacent layers in dolomite, so a C-O bond makes an angle of 6.6° with the a axis (Reeder and Wenk 1983). The net effect of cation disorder should decrease the average CO_3^{2-} group rotation angle toward zero. In the CO_3^{2-} groups, the C atom deviates slightly from the plane of the O atoms because of the difference in charge density between the Ca and Mg atoms (Lippmann 1973). A decrease in displacement of the C atom from the plane of the O atoms occurs with increasing temperature (Reeder and Wenk 1983).

Luth (2001) summarized several thermodynamic models (Navrotsky et al. 1999; Holland and Powell 1998; Martinez et al. 1996; Davidson 1994), and suggested that cation disorder is responsible for the curvature in the breakdown curve for dolomite. The results of Luth (2001) are in agreement with Martinez et al. (1996) in situ X-ray diffraction (XRD) work at lower temperatures, but not at higher temperatures where their data were extrapolated. The results of Shirasaka et al. (2002) were in reasonable agreement with those of Luth (2001), but those of Sato and Katsura (2001) were different. Navrotsky and Loucks (1977) and Putnis (1992) used the Bragg-Williams (BW) model to discuss convergent long-range cation ordering in dolomite. In addition, Luth (2001) discussed cation ordering in dolomite in terms of Landau and generalized point approximation (GPA) models.

The present study avoids the cation quench problem in dolomite, and determines the crystal structure and order parameter s from 298 to 1466 K at about 3 GPa. Our modified BW model fits experimental data quite well. Moreover, our thermodynamic description of the aragonite + magnesite ↔ dolomite reaction boundary reproduced the main qualitative features correctly.

EXPERIMENTAL METHODS

Sample

The dolomite sample used in this study was from a metamorphic carbonate complex from Eugui, Spain. Dolomite from this locality has been used in several

* E-mail: sytle.antao@stonybrook.edu

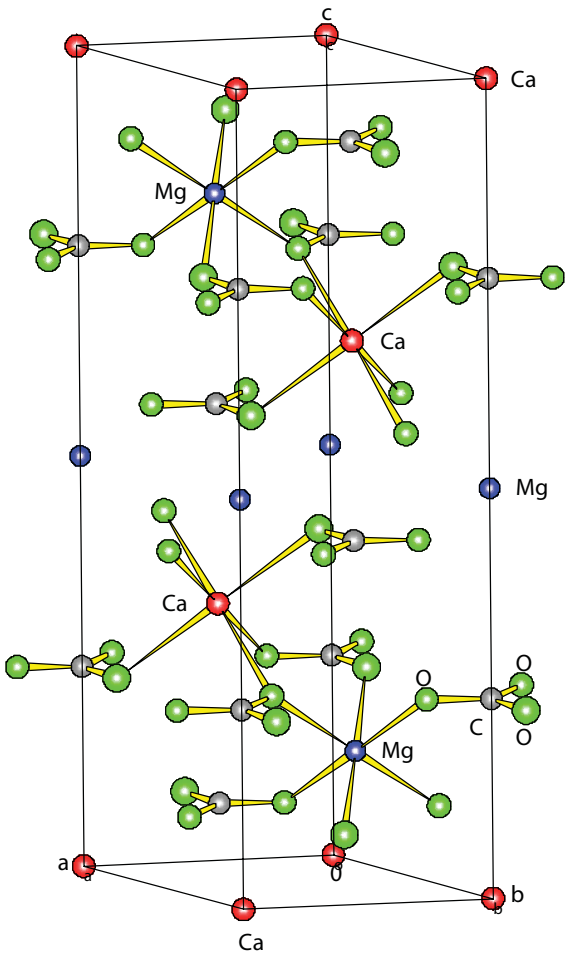

FIGURE 1. Projection of the structure of dolomite containing layers of alternating Mg^{2+} and Ca^{2+} octahedra between layers of nearly planar CO_3^{2-} groups. Only a few cation octahedra are shown for clarity. A unit cell and its orientation is indicated.

studies (e.g., Luth 2001; Navrotsky et al. 1999; Reeder and Markgraf 1986; Reeder and Wenk 1983; Reeder and Nakajima 1982). An optically clear cleavage rhomb of dolomite was ground to a fine powder under acetone in an agate mortar and pestle. The chemical composition for our Eugui dolomite sample was determined by Reeder and Wenk (1983) and is $Ca_{1.001}Mg_{0.987}Fe_{0.010}Mn_{0.002}(CO_3)_2$, which is close to the ideal formula, $CaMg(CO_3)_2$.

Synchrotron powder X-ray diffraction

In situ, powder XRD high-temperature synchrotron experiments were performed at the high-pressure beamline ID30 [λ = 0.3738(4) Å] of the European Synchrotron Radiation Facility with the Paris-Edinburgh large-volume apparatus (Besson et al. 1992). The sample was loaded in a gold capsule, which was crimped shut. The pressure was increased to about 3 GPa to seal the gold capsule and prevent decarbonation by maintaining the confining CO_2 pressure. Data were collected as the temperature was increased from 298 K to a maximum of about 1466 K on heating and on cooling to room temperature. Pressure and temperature data were obtained by cross-calibration techniques (Crichton and Mezouar 2002), using the equation of state of the capsule materials: gold (Anderson et al. 1989) and hexagonal boron nitride (Le Godec et al. 2000). In the present study, the errors in pressure and temperature are estimated to be about 0.2 GPa and 50 K, respectively. Diffraction data were collected on a MarResearch Mar345 image-plate detector with 100 micrometer resolution after calibration of detector distortion and sample-detector distance using NBS660a LaB_6 powder (a = 4.1569 Å) with Fit2D (Hammersley et al. 1995). The two-dimensional images were integrated to produce conventional 2θ-I patterns with Fit2D (Hammersley et al. 1996). Use of a multi-channel collimator significantly reduced the background contribution from the high-pressure cell assembly (Mezouar et al. 2002). X-ray data were collected to a maximum 2θ of about 27.5° [(sinθ/λ) < 0.64/Å].

RESULTS

The powder XRD data were analyzed with the Rietveld method implemented in the *GSAS* and *EXPGUI* programs (Larson and Von Dreele 2000; Toby 2001). The starting atomic coordinates, cell parameters, isotropic displacement factors, and space group, $R\bar{3}$ [origin at $\bar{3}$], were taken from Reeder and Wenk (1983). Each cation site was constrained to be fully occupied by Ca^{2+} and Mg^{2+} cations. The structure of dolomite refined quite well at different temperatures as indicated by the R values (Fig. 2; Table 1). In the present study, we are interested in the values of the order parameter s obtained by structure refinement at different temperatures (Table 1). Therefore, other structural details for dolomite are given in Table 2[1] (positions, isotropic displacement

[1]For a copy of Table 2, document item AM-04-066, contact the Business Office of the Mineralogical Society of America (see inside front cover of recent issue) for price information. Deposit items may also be available on the American Mineralogist web site at http://www.minsocam.org.

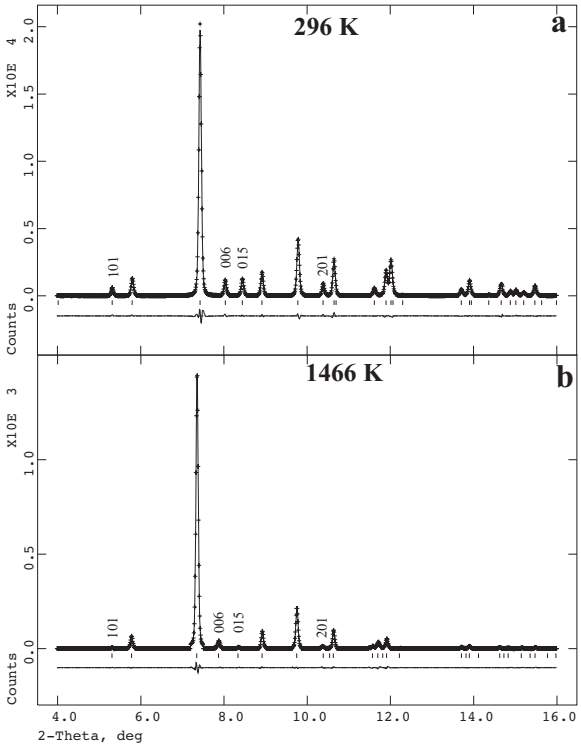

FIGURE 2. Synchrotron powder X-ray diffraction traces for dolomite (**a**) at room pressure and temperature and (**b**) at 3 GPa and 1466 K, together with the calculated (continuous line) and observed (crosses) profiles. The difference curve ($I_{obs} - I_{calc}$) that is plotted at the bottom is on the same scale. The short vertical lines indicate allowed reflection positions. The ordering reflections: 101, 015, and 201 have weak intensities but are still present in the trace at 1466 K, where s = 0.12(5) indicating incomplete $R\bar{3} \leftrightarrow R\bar{3}c$ transformation.

TABLE 1. Cell, order parameters, and Rietveld statistics at various temperatures for dolomite

T/K	a (Å)	c (Å)	c/a	V (Å^3)	x_{Ca}	s	Ratio*	R_p†	R_F^2†
296	4.8072(1)	16.0048(4)	3.3293	320.31(1)	1.000(8)	1.00(2)	1.13	0.0451	0.0575
630	4.7924(2)	15.8119(9)	3.2994	314.50(3)	0.995(8)	0.99(2)	1.24	0.0554	0.0553
675	4.7918(2)	15.8283(9)	3.3032	314.75(2)	0.991(8)	0.98(2)	1.21	0.0517	0.0488
809	4.7917(1)	15.8816(7)	3.3144	315.79(2)	0.982(8)	0.96(2)	1.21	0.0439	0.0436
925	4.7925(1)	15.9312(6)	3.3242	316.88(2)	0.971(7)	0.94(1)	1.24	0.0439	0.0456
999	4.7938(1)	15.9652(5)	3.3304	317.73(1)	0.965(7)	0.93(1)	1.10	0.0425	0.0503
1039	4.7941(1)	15.9868(5)	3.3347	318.20(1)	0.975(7)	0.95(1)	1.10	0.0444	0.0583
1074	4.7945(1)	16.0087(5)	3.3390	318.69(1)	0.967(7)	0.93(1)	1.05	0.0445	0.0595
1070	4.7942(1)	16.0061(5)	3.3386	318.60(1)	0.971(7)	0.94(1)	1.18	0.0458	0.0555
1106	4.7944(1)	16.0212(4)	3.3417	318.93(1)	0.949(8)	0.90(2)	1.10	0.0444	0.0393
1142	4.7956(1)	16.0405(4)	3.3448	319.47(1)	0.938(5)	0.88(1)	1.13	0.0494	0.0636
1171	4.7965(1)	16.0559(4)	3.3474	319.90(1)	0.944(8)	0.89(2)	1.10	0.0446	0.0355
1205	4.7985(1)	16.0815(5)	3.3514	320.68(1)	0.923(7)	0.85(1)	1.11	0.0565	0.0529
1234	4.8009(1)	16.1069(4)	3.3550	321.50(1)	0.917(5)	0.83(1)	0.99	0.0532	0.0657
1265	4.8039(1)	16.1397(4)	3.3597	322.56(1)	0.900(5)	0.80(1)	0.96	0.0481	0.0646
1292	4.8035(1)	16.1468(4)	3.3615	322.65(1)	0.878(6)	0.76(1)	0.91	0.0445	0.0531
1320	4.8055(1)	16.1791(4)	3.3668	323.57(1)	0.872(6)	0.74(1)	0.79	0.0461	0.0661
1346	4.8111(1)	16.2511(5)	3.3778	325.77(1)	0.830(6)	0.66(1)	0.83	0.0454	0.0412
1362	4.8084(2)	16.2802(7)	3.3858	325.99(2)	0.865(13)	0.73(3)	0.54	0.0281	0.0536
1394	4.8090(1)	16.2621(6)	3.3816	325.69(2)	0.832(13)	0.66(3)	0.80	0.0365	0.0633
1400	4.8089(1)	16.2901(7)	3.3875	326.25(2)	0.772(12)	0.54(2)	0.57	0.0326	0.0461
1443	4.8081(1)	16.2756(5)	3.3850	325.85(2)	0.613(10)	0.23(2)	0.69	0.0141	0.0254
1466	4.8072(1)	16.3354(6)	3.3981	326.93(2)	0.562(24)	0.12(5)	0.21	0.0123	0.0167

* Ratio = I_{015}/I_{006}.
† R_p = pattern R factor = $\Sigma|(I_o - I_c)|/\Sigma I_o$ and R_F^2 = R-structure factor based on observed and calculated structure amplitudes = $\Sigma|(F_o^{1/2} - F_c^{1/2})|/\Sigma F_o^{1/2}$.

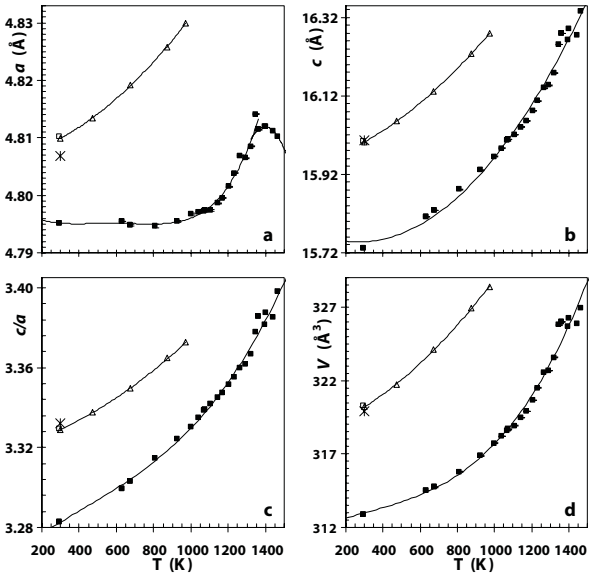

FIGURE 3. Variation of dolomite cell parameters at about 3 GPa with temperature (solid square): (**a**) a vs. T, (**b**) c vs. T, (**c**) c/a vs. T and (**d**) V vs. T. Triangles are data from Reeder and Markgraf (1986) at room pressure and crosses are data from Reeder and Wenk (1983) at room pressure and temperature. Open squares represent our data at room pressure and temperature.

parameters, and bond distances).

The room-temperature and pressure cell parameters are in agreement with those of Reeder and Markgraf (1986) and Reeder and Wenk (1983) (Fig. 3; Table 1). In the present study, the c/a ratio and volume increase smoothly with temperature and show no structural discontinuity that would indicate a phase transition (Fig. 3). Reeder and Markgraf (1986) observed a smooth increase in the cell parameters at room pressure and temperature up to 873 K, and the trend we observed is similar except that our data were collected at about 3 GPa, so our starting cell parameters are lower (Fig. 3).

The s obtained by Rietveld structure refinement is more reliable than the Schultz-Güttler (1986) intensity method where the ratio of intensities of reflections 015 and 006 is used as a measure of s. Luth (2001) indicated that the uncertainty in s using the intensity method is at least 8%, and it may be higher if preferred orientation, re-ordering on quenching, or non-equilibrium are present. Therefore, s obtained by the intensity method should be considered qualitative (Luth 2001). If we plot our intensity ratio from Table 1, considerable scatter is observed (not shown), indicating further the unreliability of this method.

ORDER PARAMETER, S

The order parameter $s = 1$ for fully ordered dolomite, and s changes when the temperature is high enough to cause exchange of Ca^{2+} and Mg^{2+} between the two octahedral cation sites (Fig. 4a). At 809 K, $s = 0.96(2)$, and at 1234 K, $s = 0.83(1)$ where the disorder is significant and increases further to the maximum temperature studied [$T = 1466$ K, $s = 0.12(5)$].

The s values of Reeder and Wenk (1983) represent maximum values of cation ordering at their respective equilibration temperatures as they used quenched samples. Therefore, our in situ data contain more disorder (lower s values) at similar temperatures compared to Reeder and Wenk (1983; our Fig. 4a), as cation ordering in dolomite is unquenchable. Reeder and Wenk (1983) indicated that $s = 0$ at about 1423 K (= T_c) and about 20 Kbars, which was confirmed by Luth (2001) using quenched samples and different pressures. However, in the present study, $s = 0.12(5)$ at about 1466 K and 3GPa. At $s = 0.12$ and $s = 0$, there is no significant difference in temperature as the curve drops almost vertically (Fig. 4a), therefore T_c is taken to be 1466 K at $s = 0$. Despite the different pressures used in these studies, the T_c is nearly the same in all.

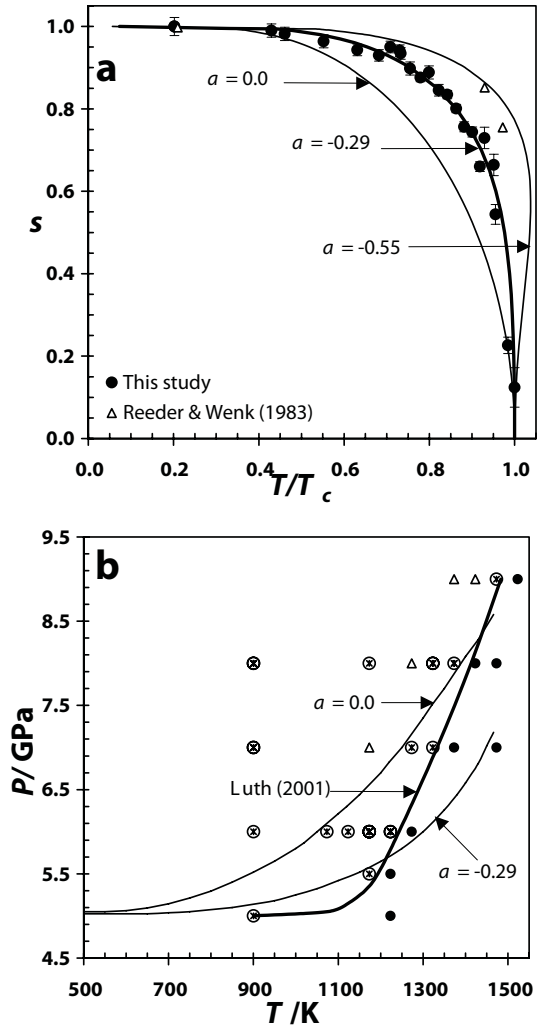

FIGURE 4. (**a**) Thermodynamic model for dolomite with a = 0.0, –0.29, and –0.55. (**b**) Comparison of our thermodynamic model for a = 0.0 and –0.29 with the experimental P-T boundary of Luth (2001; and his data points).

THERMODYNAMIC MODEL

Cation disorder in dolomite

The cation lattice in completely ordered dolomite can be regarded as consisting of two interpenetrating sub-lattices, denoted α and β, with the α sub-lattice occupied by Ca^{2+} ions and the β sub-lattice containing Mg^{2+} ions. At elevated temperatures, exchange of Ca^{2+} and Mg^{2+} ions occurs between these sub-lattices, as described in terms of the long-range order parameter s, defined as

$$s = 2x^{\alpha}_{Ca} - 1 \quad (1)$$

where x^{α}_{Ca} is the mole fraction of Ca^{2+} ions on the α sub-lattice. The value of s varies between 1 (complete order) and 0 (complete disorder), although mathematically this range can be extended down to –1, where the labels "α" and "β" distinguishing the sub-lattices have effectively been interchanged. Physically, a state characterized by order parameter s is indistinguishable from one corresponding to $-s$.

From a thermodynamic point of view, this system shows a strong resemblance to binary alloys, which suggests a description in terms of the mean-field Bragg-Williams (BW) model, with the molar configurational entropy of disordering given as (see Navrotsky and Loucks 1977; Putnis 1992):

$$\bar{S}_d(s) = \mathrm{R}[2\ \ln 2 - (1+s)\ln(1+s) - (1-s)\ln(1-s)]. \quad (2)$$

To obtain the molar enthalpy of disordering, $\bar{H}_d(s)$, the BW treatment makes use of a regular solid-solution model, which leads to

$$\bar{H}^{BW}_d(s) = N_A w(1-s^2) \quad (3)$$

with N_A the Avogadro constant and w (>0) a constant interaction parameter pertaining to nearest-neighbor contacts.

We propose to augment $\bar{H}^{BW}_d(s)$ with an extra term, proportional to $(s^4 - 1)$. A likely source of this contribution to the energy of disordering can be identified from inspection of the average rotation of the CO_3^{2-} anion groups with varying s, which is attributed to the size difference between Ca^{2+} and Mg^{2+} (see Fig. 1). At s = 1 (or s = –1), one of the C-O bonds makes an angle of θ = 6.6° with the a axis of a unit cell, whereas for s = 0, the same bond aligns with this edge (Reeder and Wenk 1983). If the CO_3^{2-} groups were to rotate collectively through the same angle θ, the energy of the lattice should vary periodically, with a periodicity of 60°. The average angle θ is a function of s so that the order-disorder process may be accompanied by a variation in strain and a concomitant change in elastic energy, which must be an even function of s. Here, only contributions proportional to s^2 and s^4 will be retained. A similar generalized BW model was proposed for the description of the antiferroelectric phase transition in titanite (Hayward et al. 2000).

The molar free energy of disordering in dolomite, $\bar{G}_d = \bar{H}_d - T\bar{S}_d$, can thus be written as follows:

$$\bar{G}_d(T; s) = \mathrm{R}T_c[1 - s^2 + {}^1/_2\, a(s^4 - 1) - (T/T_c)\ \{2\ \ln 2 - (1+s)\ln(1+s) - (1-s)\ln(1-s)\}] \quad (4)$$

defining the "critical temperature" $T_c = w/k$, with k the Boltzmann constant, and w is expected to contain a contribution due to strain. Note that no terms containing odd powers of s appear in Equation 4 because of the symmetry constraint $\bar{G}_d(T; s) = \bar{G}_d(T; -s)$. At a given temperature T, the order parameter s follows from the condition of internal equilibrium, $\partial\bar{G}_d(T; s)/\partial s = 0$, which, using Equation 4, gives

$$\frac{T(s)}{T_c} = \frac{s(1 - as^2)}{\tanh^{-1} s} \quad (5)$$

which simplifies to the usual BW result if a = 0. Analysis of Equation 5 shows that the critical temperature $T_c = T(0)$ marks a $R\bar{3} \leftrightarrow R\bar{3}c$ second-order phase transition to disordered dolomite only if $a \geq -1/3$. For $a < -1/3$, a "hump" appears on the T vs. s curve. This hump signals a first-order phase transition (and the possibility of coexistence of partially ordered and fully disordered

dolomite) as well as attendant hysteresis in the order parameter as T is scanned back and forth between T_c and the maximum temperature of metastability in the ordered phase. However, no such observations have been reported for dolomite.

A characteristic feature of second-order phase transitions is the occurrence of a discontinuous drop in the molar heat capacity ($\Delta\overline{C}_P$) at T_c. In this case, the magnitude of this discontinuity is predicted, based on Equations 4 and 5, to be

$$\Delta\overline{C}_P\,(T_c) = 3\mathrm{R}/(1 + 3a). \quad (6)$$

Our data on ordering in dolomite (acquired at $P \sim 3$ GPa, where $T_c = 1466$ K) shows good agreement with theory upon setting $a = -0.29$ (see Fig. 4a, where the BW curve is also shown for comparison, as well as a curve with $a = -0.55$, which exhibits the aforementioned hump). This value implies a maximum enthalpy of disordering, $\overline{H}_d(0) = \mathrm{R}T_c(1 - {}^1/_2\,a) \sim 13.96$ kJ/mol and $\Delta\overline{C}_P(T_c) \sim 192$ J/K mol. It is interesting to note that based on a calorimetric study, Navrotsky and Capobianco (1987) found the same value ($\overline{H}_d(0) = 13.94$ kJ/mol) for anhydrous coarse grained Eugui dolomite. However, in a later study, Navrotsky et al. (1999) reported $\overline{H}_d(0) = 33 \pm 6$ kJ/mol for a relatively poorly crystalline disordered dolomite precipitated from aqueous solution.

Effect of cation disorder on dolomite reaction boundary

A potentially important application of the fundamental result given by Equation 4 is presented by the transformation:

$$\mathrm{CaMg(CO_3)_2}\ \text{(dolomite)} \leftrightarrow \mathrm{CaCO_3}\ \text{(aragonite)} + \mathrm{MgCO_3}\ \text{(magnesite)}. \quad (7)$$

The equilibrium condition for this reaction can be written in the form

$$\overline{G}_{\mathrm{dol}}(T, P; s) = \overline{G}_{\mathrm{ar}}(T, P) + \overline{G}_{\mathrm{mag}}(T, P) \quad (8)$$

where the $\overline{G}$ values are molar free energies ("chemical potentials") such that

$$\overline{G}_{\mathrm{dol}}(T, P; s) = \overline{G}_{\mathrm{dol}}(T, P; s = 1) + \overline{G}_{\mathrm{d}}(T; s). \quad (9)$$

Equation 8 gives a description of the reaction boundary in the phase diagram of dolomite for the univariant equilibrium 7. In differential form, Equation 8 is equivalent to the Clapeyron equation:

$$\frac{dP}{dT} = \frac{\Delta\overline{S}_{rxn}}{\Delta\overline{V}_{rxn}} \quad (10)$$

with $\Delta\overline{S}_{rxn} = \overline{S}_{\mathrm{dol}} - \overline{S}_{\mathrm{ar}} - \overline{S}_{\mathrm{mag}}$ and similarly $\Delta\overline{V}_{rxn} = \overline{V}_{\mathrm{dol}} - \overline{V}_{\mathrm{ar}} - \overline{V}_{\mathrm{mag}}$.

The experimental reaction boundary is shown in Figure 4b (Luth 2001). It has been suggested that its shape could be accounted for in terms of cation disordering. Data on volume changes accompanying the transformation in Equation 7 show a weak pressure dependence of $\Delta\overline{V}_{rxn}$ along the boundary (Luth 2001).

The horizontal tangent that prevails for $T < 1100$ K indicates that $\Delta\overline{S}_{rxn} \cong 0$ as long as $s \sim 1$ so that vibrational contributions to $\Delta\overline{S}_{rxn} = \Delta\overline{H}_{rxn}/T$ must cancel each other for the most part. As a first approximation, we shall therefore assume that $\Delta\overline{V}_{rxn} \sim$ constant based on data from Luth (2001), and $\Delta\overline{S}_{rxn} \cong \overline{S}_d$. Equation 10 can then be integrated, after a change of integration variable from T to s, using $dT = dsT'(s)$ together with Equations 2 and 5, to give:

$$P(s) = \mathrm{P}_0 + (\mathrm{R}/\Delta\overline{V}_{rxn}) \times\left[2T(s)\ln 2 + \int_s^1 du T'(u)\big((1+u)\ln(1+u) + (1-u)\ln(1-u)\big)\right] \quad (11)$$

(where the integration constant P_0 is taken to be equal to 5 GPa).

Equations 5 and 11 together constitute a parameterization of the P vs. T curve, which is plotted in Figure 4b, assuming $\Delta\overline{V}_{rxn} = 0.13$ J/mol bar, for both $a = -0.29$ and $a = 0$. Either theoretical curve provides a poor fit to the experimental data, even though each tends to reproduce the main qualitative features correctly. Correction for the weak pressure dependence of $\Delta\overline{V}_{rxn}$ is not expected to lead to significant improvement that, within the present theoretical framework, would leave the option of an explicit dependence of $\overline{\mathrm{G}}_d$ on pressure, which would have to enter Equation 4 via a and/or T_c. We are presently trying to obtain these important experimental data to further improve on this aspect of the model for dolomite.

To summarize, we have determined the cation disorder s in dolomite at about 3 GPa and temperatures to about 1466 K using Rietveld structure refinement, which is more reliable than the intensity measurement method of Schultz-Güttler (1986). We have modeled the cation disorder in dolomite using a modified BW model that fits our experimental data quite well, and our value for the enthalpy for complete disorder in dolomite agrees with the calorimetric data of Navrotsky and Capobianco (1987). We expect our thermodynamic model to be applicable to other dolomite-type materials, e.g., $\mathrm{CdMg(CO_3)_2}$, and work is in progress on these materials as well.

ACKNOWLEDGMENTS

We thank R.J. Reeder and J. Chen for useful discussions. We thank the reviewers, Alexandra Navrotsky and Robert Luth, and the editor, Robert Dymek, for useful comments. The dolomite sample was provided courtesy of R.J. Reeder. This study was supported by a NSF grant EAR-0125094 to J.B.P. The experimental work was performed at ID30 of the ESRF, no. HS2130.

REFERENCES CITED

Anderson, O.L., Isaak, D.G., and Yamamoto, S. (1989) Anharmonicity and the equation of state for gold. Journal of Applied Physics, 65, 1534–1543.

Besson, J.M., Nelmes, R.J., Hamel, G., Loveday, J.S., Weill, G., and Hull, S. (1992) Neutron powder diffraction above 10 GPa. Physica B, 180, 907–910.

Crichton, W.A. and Mezouar, M. (2002) Noninvasive pressure and temperature estimation in large-volume apparatus by equation-of-state cross-calibration. High Temperatures-High Pressures, 34, 235–242.

Davidson, P.M. (1994) Ternary Iron, Magnesium, Calcium Carbonates—a thermodynamic model for dolomite as an ordered derivative of calcite-structure solutions. American Mineralogist, 79, 332–339.

Ferrario, M., Lyndenbell, R.M., and McDonald, I.R. (1994) Structural fluctuations and the order disorder phase transition in calcite. Journal of Physics: Condensed Matter, 6, 1345–1358.

Hammersley, A.P., Svensson, S.O., Thompson, A., Graafsma, H., Kvick, A., and Moy, J.P. (1995) Calibration and correction of distortion in two-dimensional detector systems. Review of Scientific Instruments, 66, 2729–2733.

Hammersley. A.P., Svensson, S.O., Hanfland, M., Fitch, A.N., and Hausermann, D. (1996) Two-dimensional detector software: from real detector to idealised image or two-theta scan. High Pressure Research, 14, 235–248.

Hayward, S.A., Cerro, J. del, and Salje, E.K.H. (2000) Antiferroelectric phase transition in titanite: excess entropy and short range order. American Mineralogist, 85, 557–562.

Holland, T.J.B. and Powell, R. (1998) An internally consistent thermodynamic

data set for phases of petrological interest. Journal of Metamorphic Geology, 16, 309–343.

Larson, A.C. and Von Dreele, R.B. (2000) General Structure Analysis System (GSAS). Los Alamos National Laboratory Report, LAUR 86-748.

Lippmann, F. (1973) Sedimentary Carbonate Minerals. Springer-Verlag, New York.

Le Godec, Y., Martinez-Garcia, D., Mezouar, M., Syfosse, G., Itie, J.P., and Besson, J.M. (2000) Equation of state and order parameter in graphite-like h-BN under high pressure and temperature. Proceedings of AIRAPT-17: Science and Technology of High Pressure. Eds. Manghnani, M.H., Nellis, W.J., and Nicol, M.F. (Universities Press, Hyderabad, India) p. 925–928.

Luth, R.W. (2001) Experimental determination of the reaction aragonite + magnesite = dolomite at 5 to 9 GPa. Contributions to Mineralogy and Petrology, 141, 222–232.

Martinez, I., Zhang, J.Z. and Reeder, R.J. (1996) In situ X-ray diffraction of aragonite and dolomite at high pressure and high temperature: Evidence for dolomite breakdown to aragonite and magnesite. American Mineralogist, 81, 611–624.

Mezouar, M., Faure, P., Crichton, W., Rambert, N., Sitaud, B., Bauchau, S., and Blattmann, G. (2002) Multichannel collimator for structural investigations of liquids and amorphous materials at high pressures and temperatures. Review of Scientific Instruments, 73, 3570–3574.

Navrotsky, A. and Capobianco, C. (1987) Enthalpies of formation of dolomite and of magnesian calcites. American Mineralogist, 72, 782–787.

Navrotsky, A. and Loucks, D. (1977) Calculation of subsolidus phase relations in carbonates and pyroxenes. Physics and Chemistry of Minerals, 1, 109–127.

Navrotsky, A., Dooley, D., Reeder, R., and Brady, P. (1999) Calorimetric studies of the energetics of order-disorder in the system $Mg_{1-x}Fe_xCa(CO_3)_2$. American Mineralogist, 84, 1622–1626.

Putnis, A. (1992) Introduction to mineral sciences. Cambridge University Press, Cambridge.

Reeder, R.J. and Markgraf, S.A. (1986) High-temperature crystal chemistry of dolomite. American Mineralogist, 77, 795–804.

Reeder, R.J. and Nakajima, Y. (1982) The nature of ordering and ordering defects in dolomite. Physics and Chemistry of Minerals, 8, 29–35.

Reeder, R.J. and Wenk, H.R. (1983) Structure refinements of some thermally disordered dolomites. American Mineralogist, 68, 769–776.

Sato, K. and Katsura, T. (2001) Experimental investigation on dolomite dissociation into aragonite + magnesite up to 8.5 GPa. Earth and Planetary Science Letters, 184, 529–534.

Schultz-Güttler, R. (1986) The influence of disordered, non-equilibrium dolomites on the Mg-solubility in calcite in the system $CaCO_3$-$MgCO_3$. Contributions to Mineralogy and Petrology, 93, 395–398.

Shirasaka, M., Takahashi, E., Nishihara, Y., Matsukage, K., and Kikegawa, T. (2002) In situ X-ray observation of the reaction dolomite = aragonite + magnesite at 900–1300 K. American Mineralogist, 87, 922–930.

Toby, B.R. (2001) EXPGUI, a graphical user interface for GSAS. Journal of Applied Crystallography, 34, 210–221.

MANUSCRIPT RECEIVED FEBRUARY 10, 2004
MANUSCRIPT ACCEPTED MARCH 22, 2004
MANUSCRIPT HANDLED BY ROBERT DYMEK